Supporting Information

Purely Organic Light-harvesting Phosphorescence Energy Transfer by β-Cyclodextrin Pseudorotaxane for Mitochondria Targeted Imaging

Fang-Fang Shen, Yong Chen, Xianyin Dai, Hao-Yang Zhang, Bing Zhang, Yaohua Liu,

Yu Liu*

1. Synthesis and characterization of related compounds. 3
1.1. Synthesis of CD-PY 3
Figure S1. ^{1}H NMR spectrum of CD-PY. 3
Figure S2. ^{1}C NMR spectrum of CD-PY. 4
Figure S3. HRMS (ESI) spectrum of CD-PY. 4
1.2. Synthesis of HA-ADA 4
Figure S4. ^{1}H NMR spectrum of HA-ADA. 5
2. Figures 5
Figure S5. ^{1}H-^{1}H ROESY spectrum of CD-PY in the presence of 0.5 equiv CB[8]. 6
Figure S6. ^{1}H NMR titration spectra of CD-PY in the presence of CB[7]. 6
Figure S7. UV/vis spectral changes of CD-PY upon addition of CB[7]. 7
Figure S8. UV/vis spectral changes of CD-PY upon addition of CB[8]. 7
Figure S9. Fluorescence lifetime curve of CD-PY and CD-PY@CB[8] at 384 nm. 8
Figure S10. Decay curve of CD-PY@CB[7] (1:1) at 510 nm. 8
Figure S11. Calorimetric titrations of injecting CD-PY solution into CB[7] solution. 9
Figure S12. Calorimetric titrations of injecting CD-PY solution into CB[8] solution. 9
Figure S13. ^{1}H NMR spectra of (a) CD-PY@CB[8] (1:0.5), (b) CD-PY@CB[8]@RhB (1:0.5:1), (c) β-CD@RhB (1:1), and (d) RhB. 10
Figure S14. ^{1}H NMR spectrum of β-CD@RhB (1:1). 10
Figure S15. Zoomed view of the ROESY spectrum of β-CD: RhB (1:1). 11
Figure S16. The geometry optimized of CD-PY@CB[8]@RhB. 11
Figure S17. Gated emission spectra of CD-PY@CB[8]@RhB (1:0.5:0.02) with or without N_2 in aqueous solution. 12
Figure S18. Normalized fluorescence and gated emission spectra of CD-PY@CB[8]@RhB (1:0.5:0.02) in aqueous solution. 12
Figure S19. Normalized phosphorescence spectra (delayed 0.1 ms) of CD-PY in solid state with different concentrations of RhB. 13
Figure S20. Decay curves of CD-PY in the presence of (a) 1%, and (a) 3% RhB in solid state (Ex =320 nm). 13
Figure S21. Fluorescence lifetime curve of CD-PY@CB[8]@RhB (1: 0.5: 0.02) aqueous solution at 384 nm. 14

Figure S22. Gated emission spectra of CD-PY@CB[8]@RhB (1:0.5:0.02) and CD-PY@RhB (1:0.02) in aqueous solution. 14
Figure S23. Gated emission spectra of CD-PY@CB[8]@RhB (1:0.5:0.02) upon the gradual addition of HA-ADA in aqueous solution. 15
Figure S24. Decay curves of (a) CD-PY@CB[8]@RhB (1:0.5:0.02), and (b) CD-PY@CB[8]@RhB@HA-ADA (1:0.5: 0.02:0.31) in water at 500 nm. 15
Table S1. Summary of all lifetimes used by different exponential decay. 16
Figure S25. Relative cell viabilities of CD-PY@CB[8]@RhB@HA-ADA (1:0.5:0.02:0.31) at different concentrations. (Concentrations in the Figure represent [CD-PY]). 16
3. Methods 16
3.1 Energy-transfer efficiency (Φ_{ET}). 17
Figure S26. Phosphorescence spectra of CD-PY@CB[8] (1:0.5) with or without RhB in water ([CD-PY] = 5×10^{-4} M, Ex = 340 nm). 17
3.2 Antenna effect. 17
Figure S27. Phosphorescence spectra of CD-PY@CB[8]@RhB (1:0.5:0.02) Under different excitation conditions in water. 18
4. References 18

Experimental section

1. Synthesis and characterization of related compounds

1.1 Synthesis of CD-PY

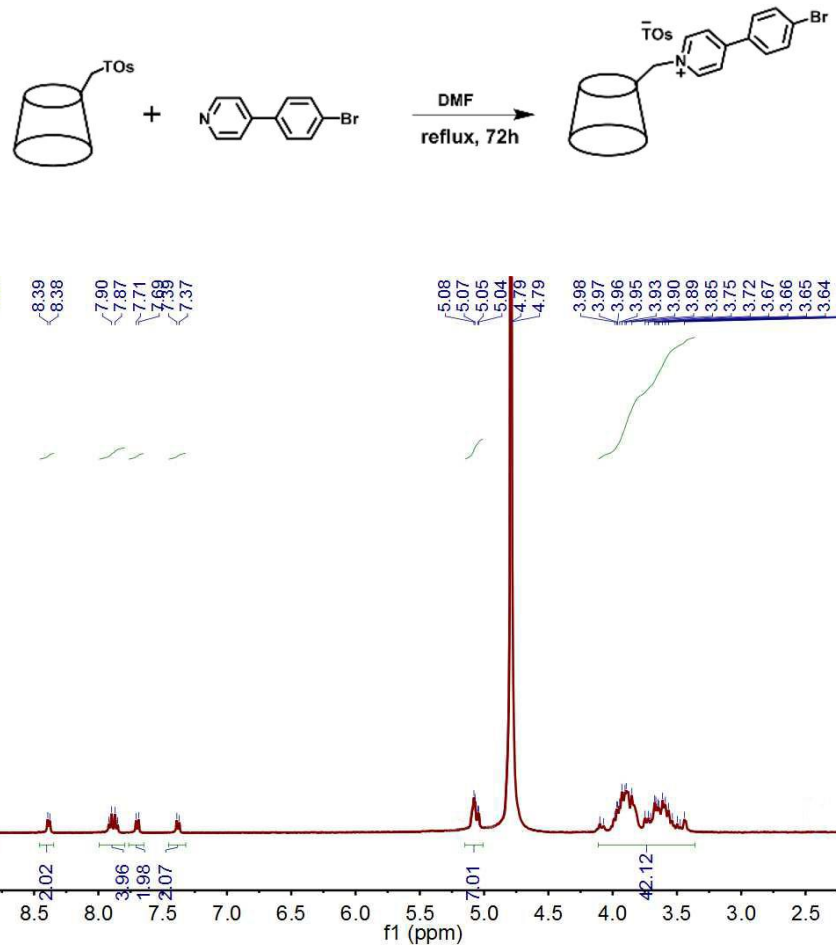

Figure S1[1]H NMR spectrum of CD-PY (D_2O, 400 MHz, 298K).

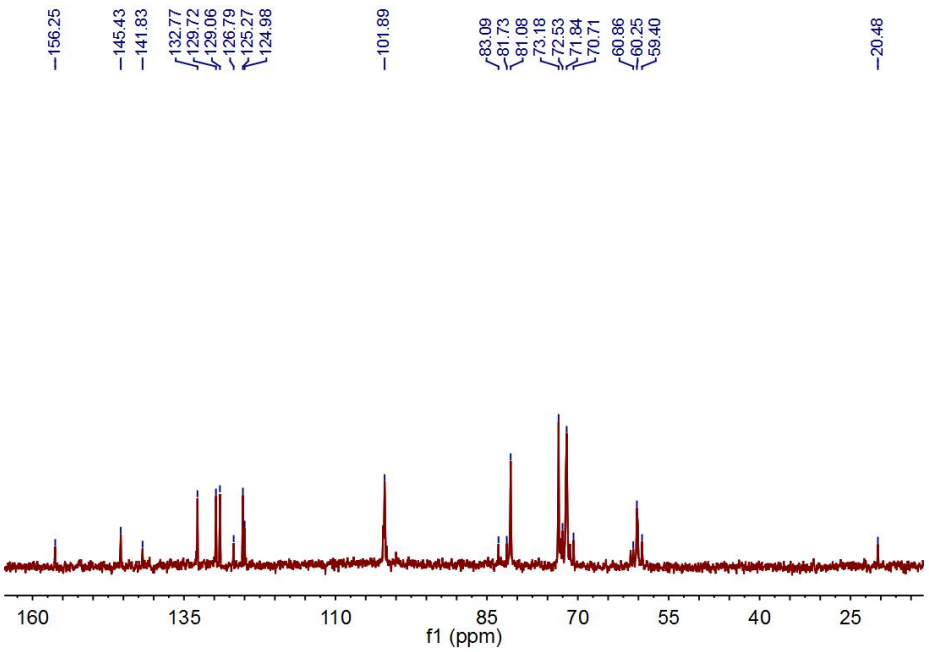

Figure S2 ^{13}C NMR spectrum of CD-PY (D_2O, 400 MHz, 298K).

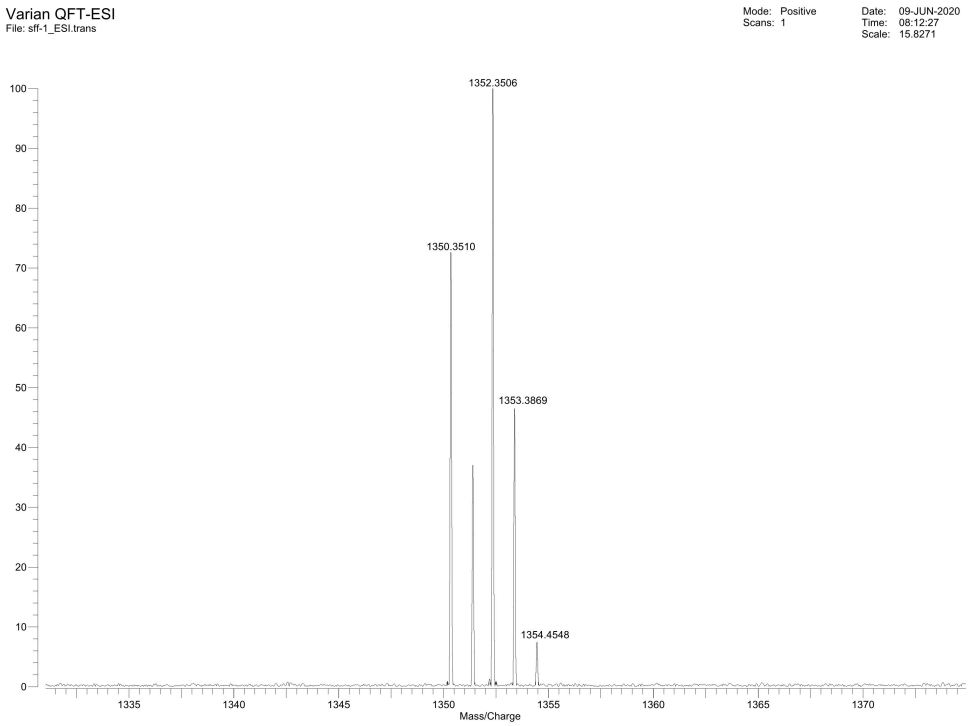

Figure S3 HRMS (ESI) spectrum of CD-PY.

1.2 Synthesis of HA-ADA

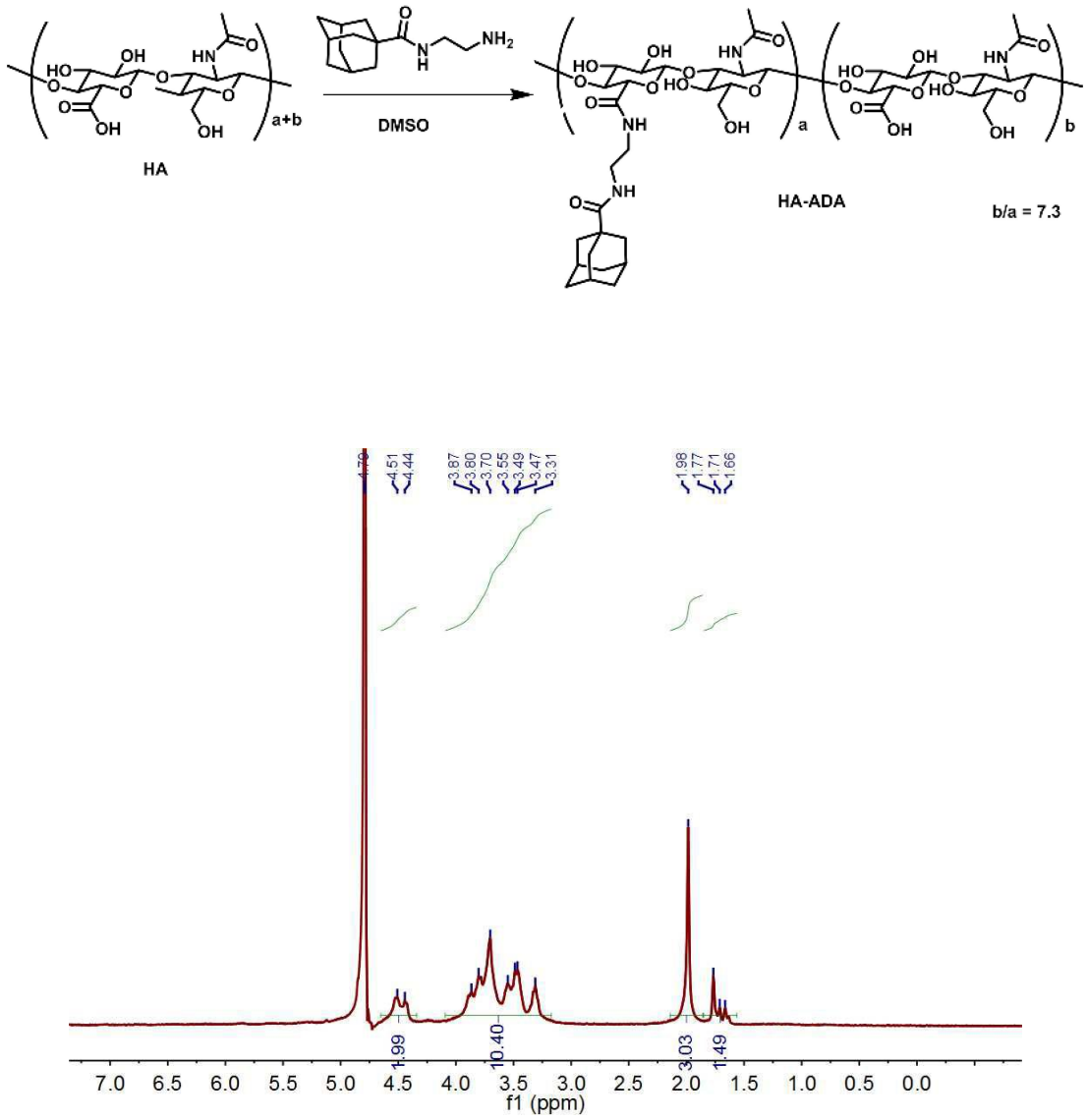

Figure S4 ^{1}H NMR spectrum of HA-ADA (D_2O, 400 MHz, 298K).

2 Figures

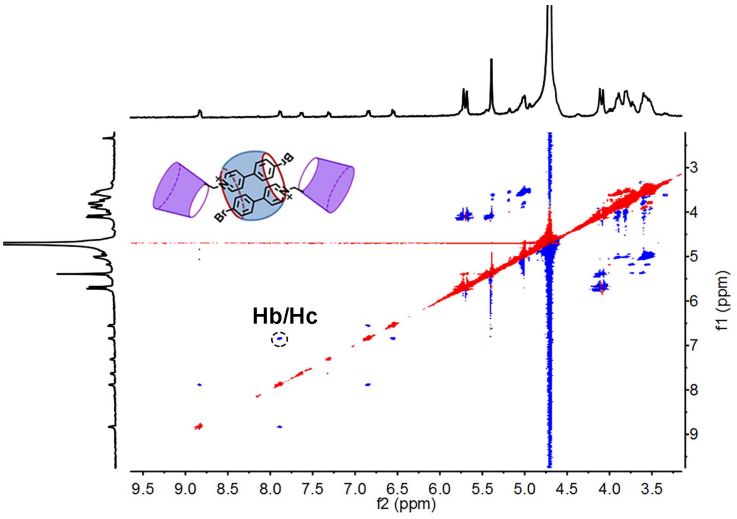

Figure S5. ^{1}H-^{1}H ROESY spectrum of CD-PY in the presence of 0.5 equiv CB[8] (400 MHz, D_2O, 298K, [CD-PY] = 1.0 mM).

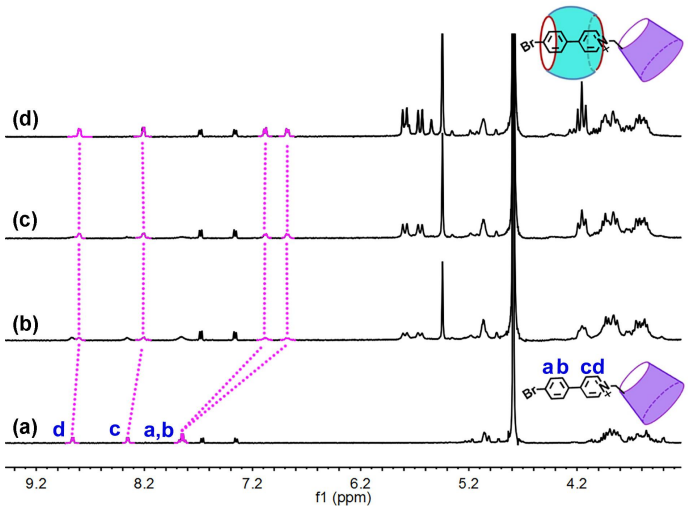

Figure S6. ^{1}H NMR titration spectra of CD-PY in the presence of (a) 0.00, (b) 0.40, (c) 0.60, (d) 1.00 equiv. of CB[7] (400 MHz, D_2O, 298K, [CD-PY] = 1.0 mM).

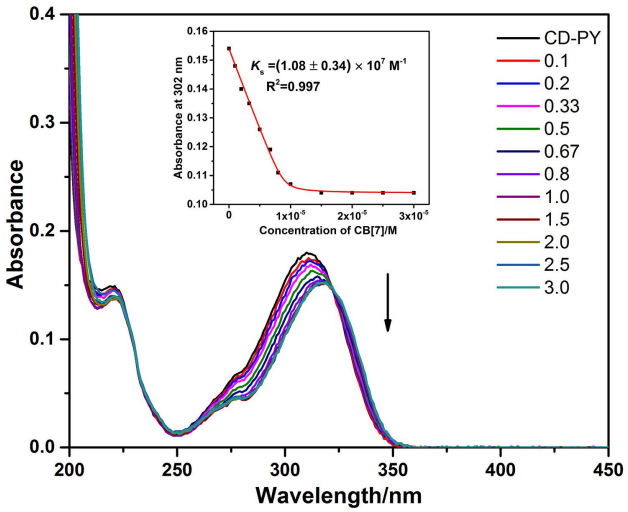

Figure S7. UV/vis spectral changes of CD-PY upon addition of CB[7]. The spectral changes were recorded in water. Inset: nonlinear least-squares analysis ("one host, one guest" mode) of the absorbance intensity changes at 302 nm used to calculate the *K*s value between CD-PY and CB[7] in water ([CD-PY] = 1.0 × 10^{-5} M, [CB[7]] = 0–3.0 × 10^{-5} M, 298 K).

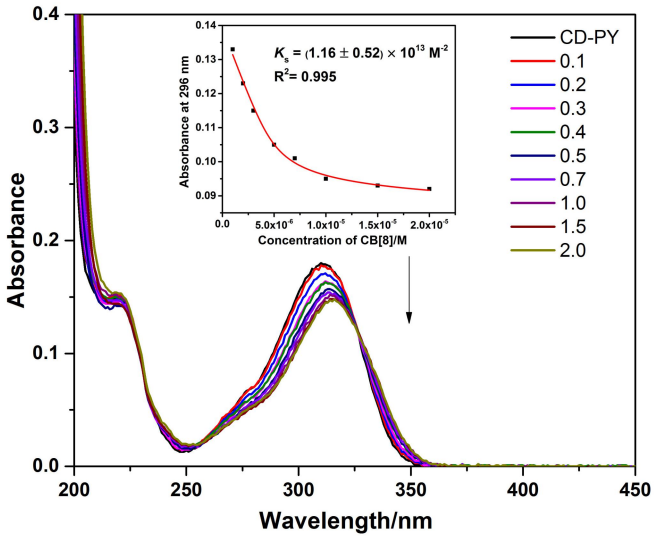

Figure S8. UV/vis spectral changes of CD-PY upon addition of CB[8]. The spectral changes were recorded in water Inset: nonlinear least-squares analysis ("one host, two guest" mode) of the absorbance intensity changes at 296 nm used to calculate the *K*s value between CD-PY and CB[8] in water ([CD-PY] = 1.0 × 10^{-5} M, [CB[8]] = 0–2.0 × 10^{-5} M, 298 K).

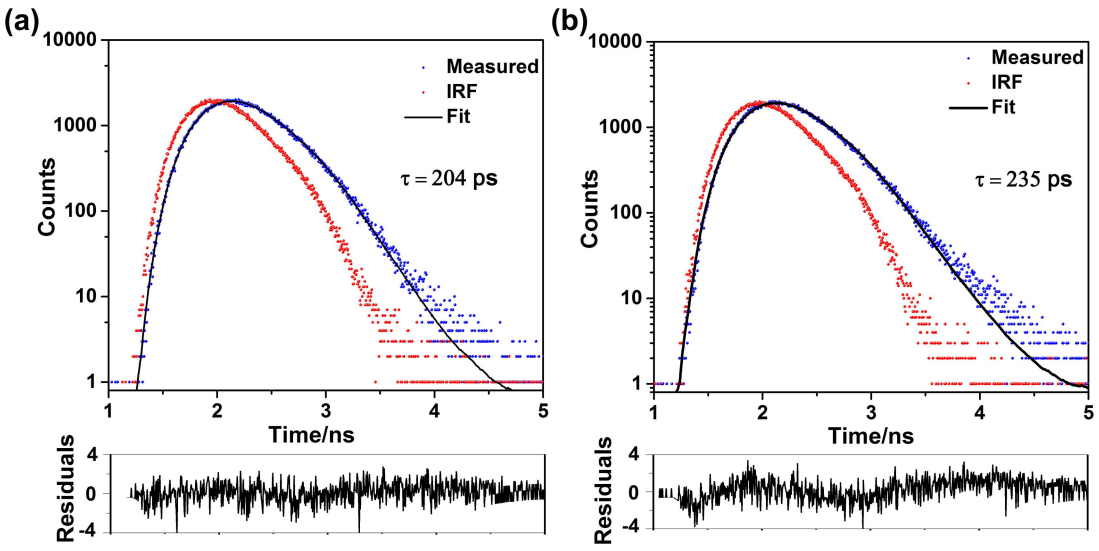

Figure S9. Fluorescence lifetime curve of CD-PY and CD-PY@CB[8] (1: 0.5) aqueous solution at 384 nm ([CD-PY] = 5.0×10^{-4} M, 298 K).

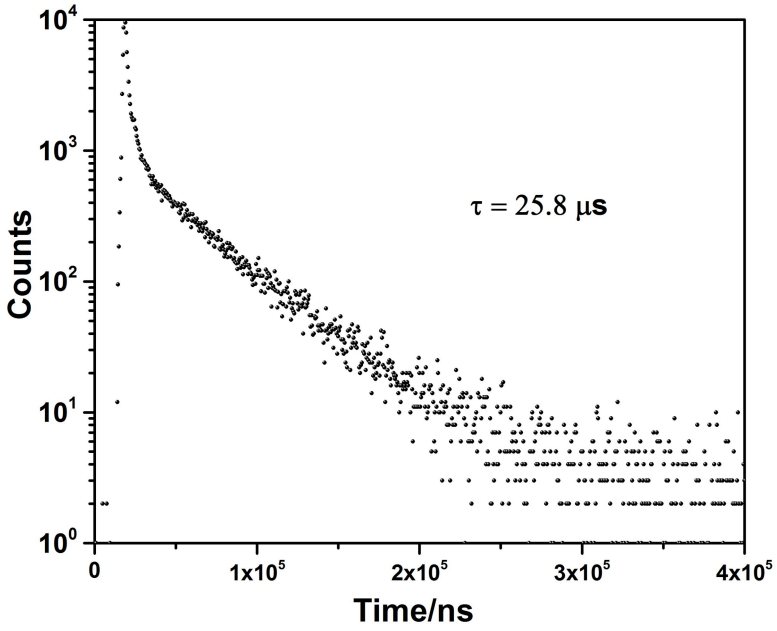

Figure S10. Decay curve of CD-PY@CB[7] (1:1) aqueous solution at 510 nm ([CD-PY] = 5.0×10^{-4} M, 298 K).

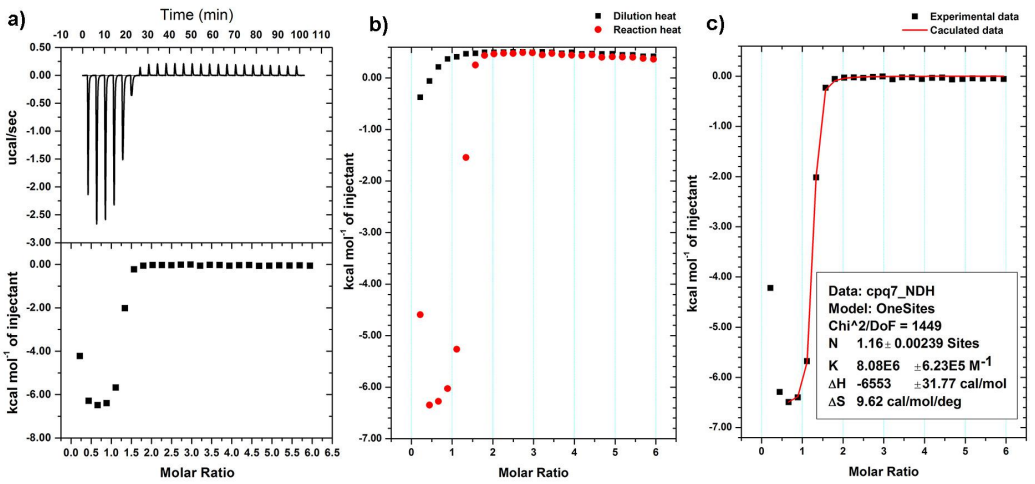

Figure S11. (A) Calorimetric titrations in aqueous solution for sequential 25 injections (10 μL per injection) of CD-PY solution (1.25 mM) injecting into CB[7] solution (0.040 mM): (a) raw data and apparent reaction heat; (b) heat effects of the dilution and of the complexation reaction; (c) "Net" heat effects fitted using the "one set of binding sites" model. The thermodynamic data in CD-PY@CB[7] complex were obtained as $K_s = (8.08 \pm 0.62) \times 10^6$ M^{-1},

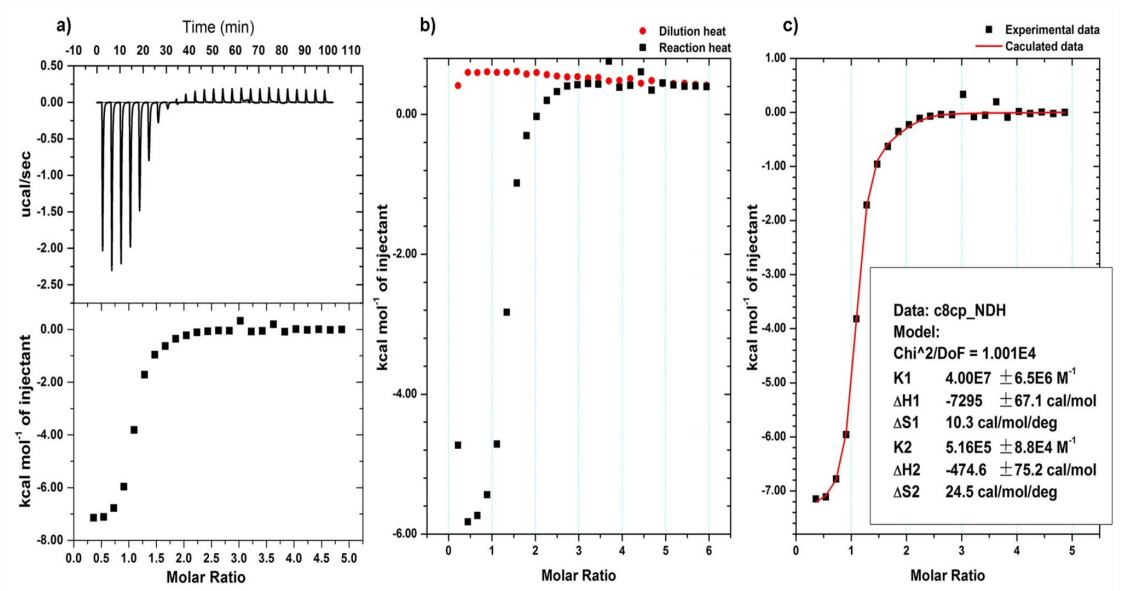

Figure S12. Calorimetric titrations in aqueous solution for sequential 25 injections (10 μL per injection) of injecting CD-PY solution (1.10 mM) into CB[8] solution (0.043 mM): (a) raw data and apparent reaction heat; (b) heat effects of the dilution and of the complexation reaction; (c) "Net" heat effects fitted using the "Sequential Binding Sites" model. The thermodynamic data in CD-PY@CB[8] complex were obtained as $K_{a1} = (4.00 \pm 0.65) \times 10^7$ M^{-1}, $K_{a2} = (5.16 \pm 0.88) \times 10^5$ M^{-1}, respectively.

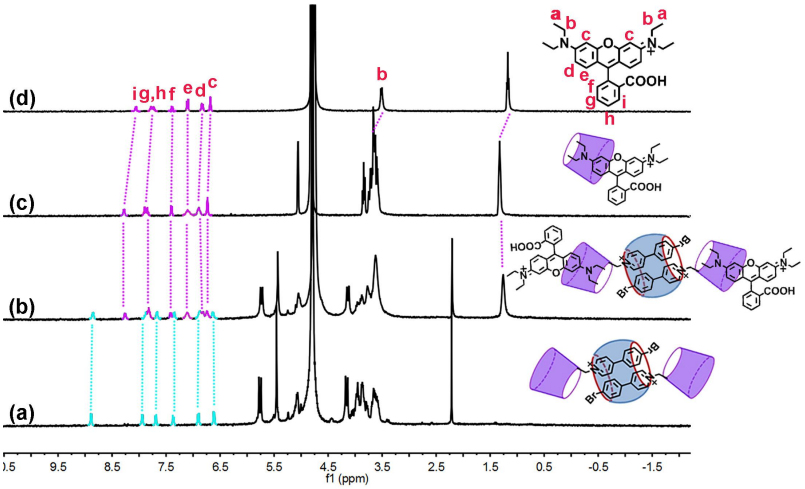

Figure S13. ^{1}H NMR spectra (400 MHz, D_2O, 298 K) of (a) CD-PY@CB[8] (1:0.5), (b) CD-PY@CB[8]@RhB (1:0.5:1), (c) β-CD@RhB (1: 1) and (d) RhB ([RhB] = 1 mM).

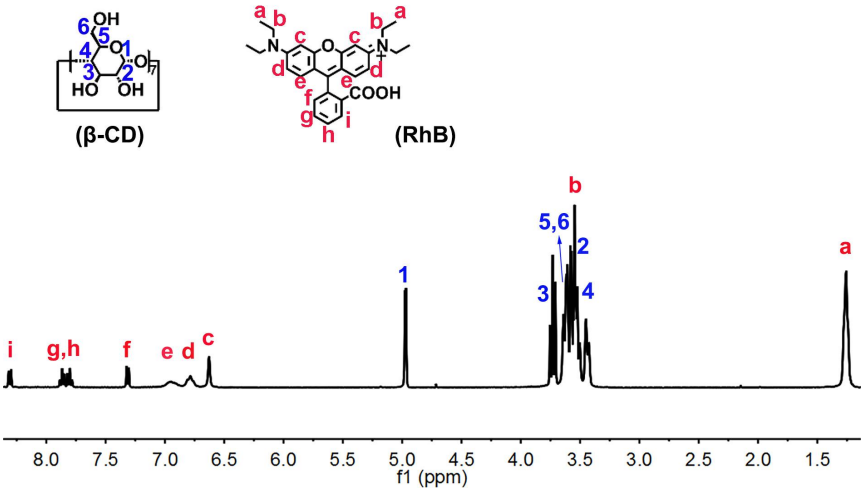

Figure S14. ^{1}H NMR spectrum of β-CD@RhB (1:1) (400 MHz, D_2O, 298 K, [β-CD] = [RhB] = 1 mM).

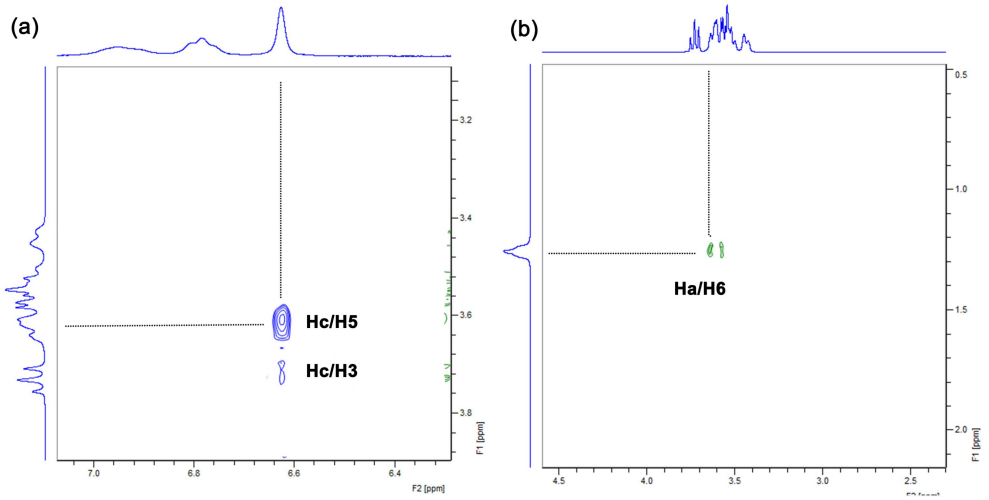

Figure S15. Zoomed view of the ROESY spectrum of β-CD@RhB (1:1) (400 MHz, D_2O, 298 K, [β-CD] = [RhB] = 1 mM).

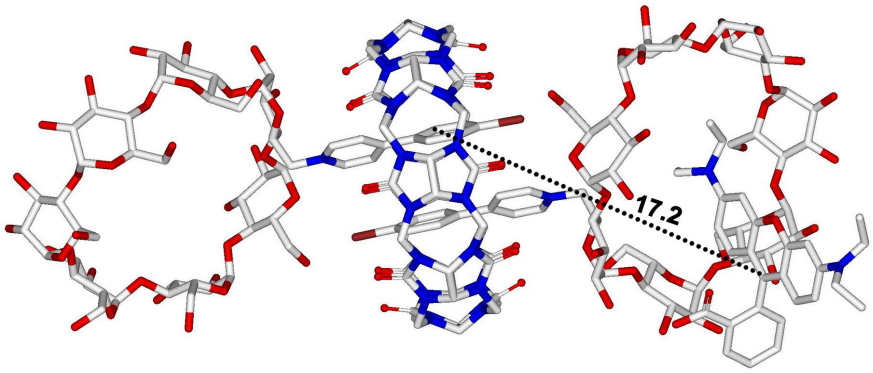

Figure S16. The geometry optimized by the molecular mechanics modelling using the universal force field[1] by Gaussian 16[2] and rendered by CYL view[3]. The distance between RhB and PY unit in the host-guest complexes was calculated to be 17.2 Å.

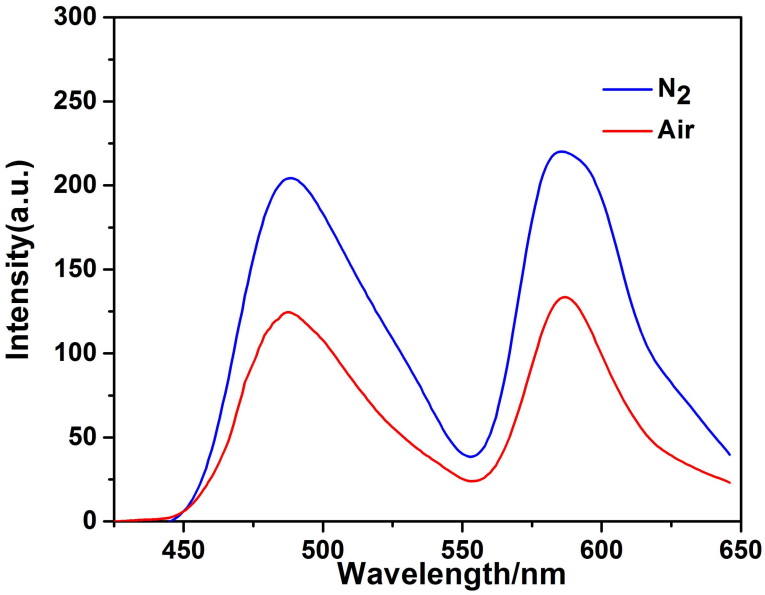

Figure S17. Gated emission spectra of CD-PY@CB[8]@RhB (1:0.5:0.02) with or without N_2 in aqueous solution (Ex =340 nm, [CD-PY]= 5×10^{-4} M, 298 K).

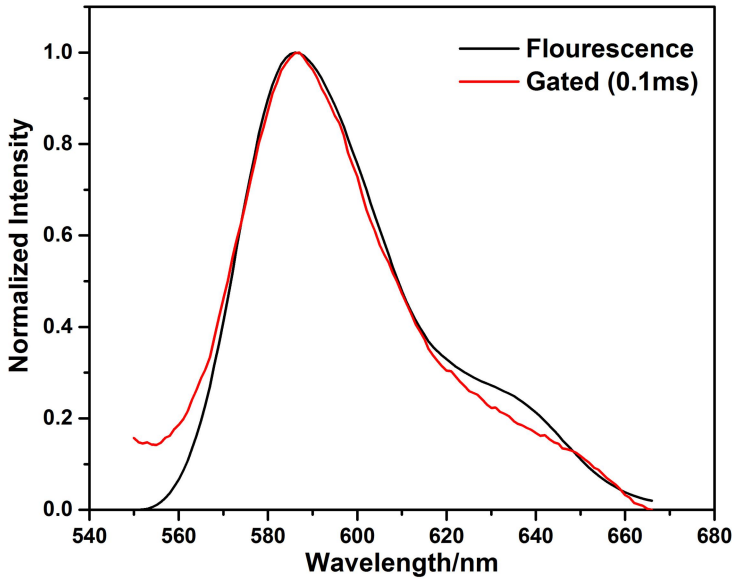

Figure S18. Normalized fluorescence and gated emission spectra of CD-PY@CB[8]@RhB in the solution (1:0.5:0.02) (Ex =340 nm, [CD-PY]= 5×10^{-4} M, 298 K).

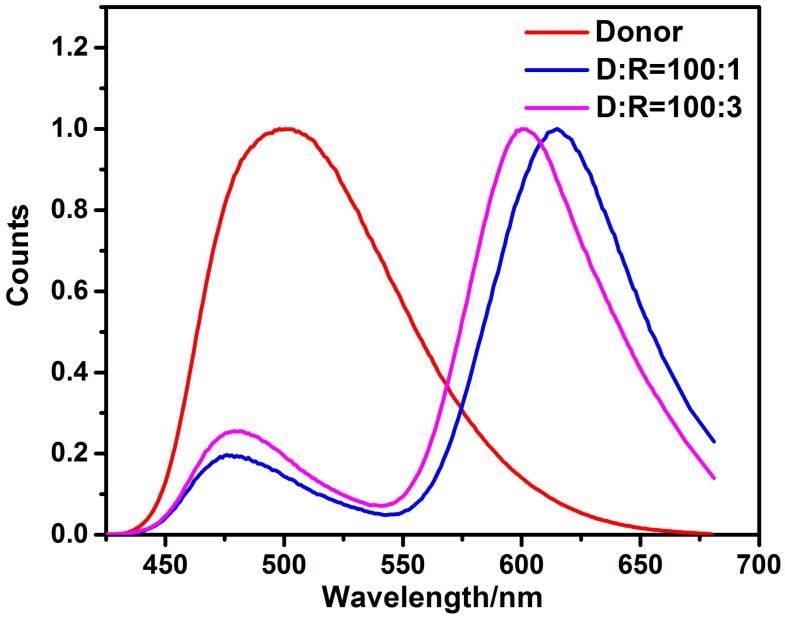

Figure S19. Normalized gated spectra (delayed 0.1 ms) of CD-PY in solid state with different concentrations of RhB (Ex =320 nm).

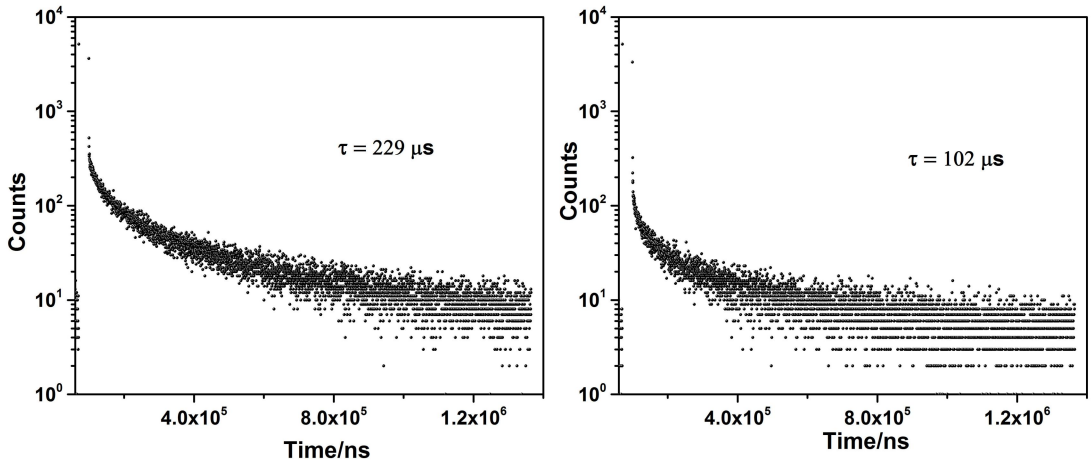

Figure S20. Decay curves of CD-PY in the presence of (a) 1%, and (a) 3% RhB in solid state (Ex =320 nm).

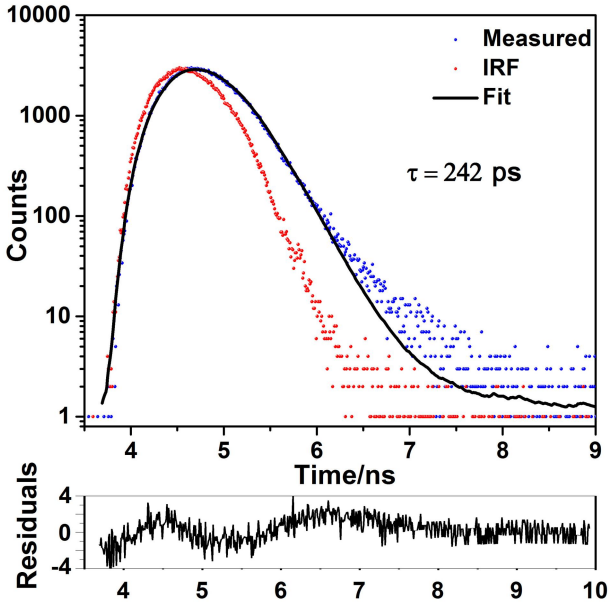

Figure S21. Fluorescence lifetime curve of CD-PY@CB[8]@RhB (1: 0.5: 0.02) aqueous solution at 384 nm ([CD-PY] = 5.0 × 10^{-4} M, 298 K)..

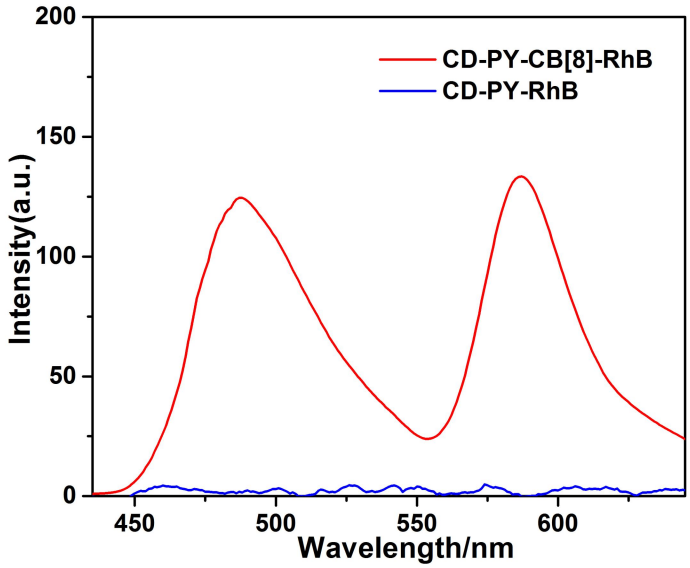

Figure S22. Gated mission spectra of CD-PY@CB[8]@RhB (1:0.5:0.02), and CD-PY@RhB (1:0.02) in aqueous solution ([CD-PY]= 5 × 10^{-4} M, Ex =340 nm, 298 K).

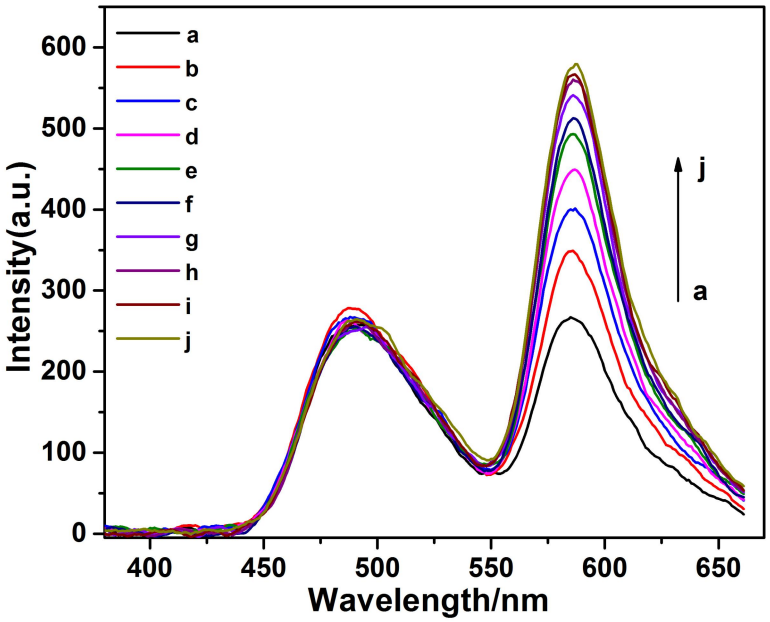

Figure S23. Gated emission spectra of CD-PY@CB[8]@RhB (1:0.5:0.02) upon the gradual addition of HA-ADA in aqueous solution ([CD-PY] = 5 × 10^{-4} M, [HA-ADA] = 0-1.55 × 10^{-4} M) at 298 K (Ex. Slit =10, Em. Slit=20).

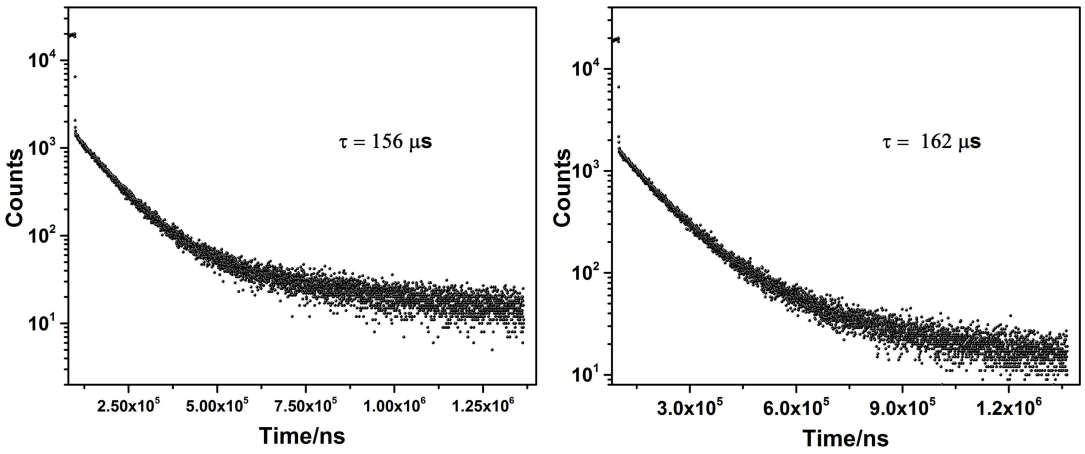

Figure S24. Decay curves of (a) CD-PY@CB[8]@RhB (1:0.5:0.02), and (b) CD-PY@CB[8]@RhB@HA-ADA (1:0.5: 0.02:0.31) in water at 500 nm, at 298 K.

Table S1. Summary of all lifetimes used by different exponential decay.

Figures	Lifetime (us) (% contribution)			
	τ1	**τ2**	**τ3**	**τ**
Fig. 2d	37.46 0.13%	405.50 84.26%	1040.62 15.62%	504
Fig. 3d	215.21 43.46%	1214.52 56.54%	-	780
Fig. 4b	0.18 0.1%	199 45.75%	365 54.15 %	289
Fig. S10	1.17 22.63%	5.73 20.94%	43.18 56.43%	25.8
Fig. S20a	42.19 24.75%	295.70 73.85%	0.13 1.40%	229
Fig. S20b	0.139 6.06%	108.59 93.94%	-	102
Fig. S24a	85 76.56%	390 23.44%	-	156
Fig. S24b	102 73.35%	324 26.65%	-	162

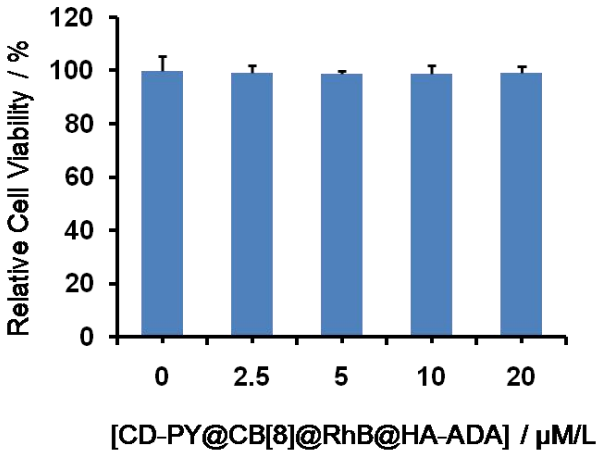

Figure S25. Relative cell viabilities of CD-PY@CB[8]@RhB@HA-ADA (1:0.5:0.02:0.31) at different concentrations. (Concentrations in the Figure represent [CD-PY]).

3. Methods

3.1 Energy-transfer efficiency (Φ_{ET})

Energy-transfer efficiency (Φ_{ET}) was calculated according to the equation (1).[4]

$$\Phi_{ET} = 1 - I_{DA}/I_D \quad (1)$$

In the equation, I_{DA} and I_D are the emission intensity of the ET donor with and without the presence of ET acceptor, respectively. The Φ_{ET} was calculated as 84% in water, measured in the condition of CD-PY@CB[8]@RhB (1:0.5:0.02), λ_{ex} = 340 nm.

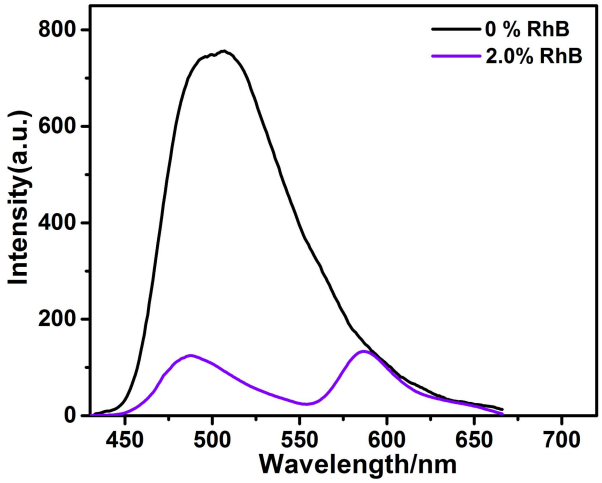

Figure S26. Phosphorescence spectra of CD-PY@CB[8] (1:0.5) with or without RhB in water ([CD-PY] = 5×10^{-4} M, Ex = 340 nm).

3.2 Antenna effect

The antenna effect under certain concentrations of donor and acceptor was calculated according to the equation (2) [5]

$$\text{Antenna effect} = \frac{I^{590\ nm}_{DA(\lambda_{ex}=340\ nm)} - I^{590\ nm}_{D(\lambda_{ex}=340\ nm)}}{I^{590\ nm}_{DA(\lambda_{ex}=550\ nm)}} \quad (2)$$

In the equation, I_{DA} (λ_{ex} = 340 nm) and I_{DA} (λ_{ex} = 550 nm) are the phosphorescence intensities of excitation of the ET donor with the presence of ET acceptor at 340 nm and direct excitation of the acceptor at 550 nm, respectively. The

antenna effect value was calculated as 36.42 in water, measured in the condition of CD-PY@CB[8]@RhB (1:0.5:0.02) (λ_{ex} = 340 nm or 550 nm).

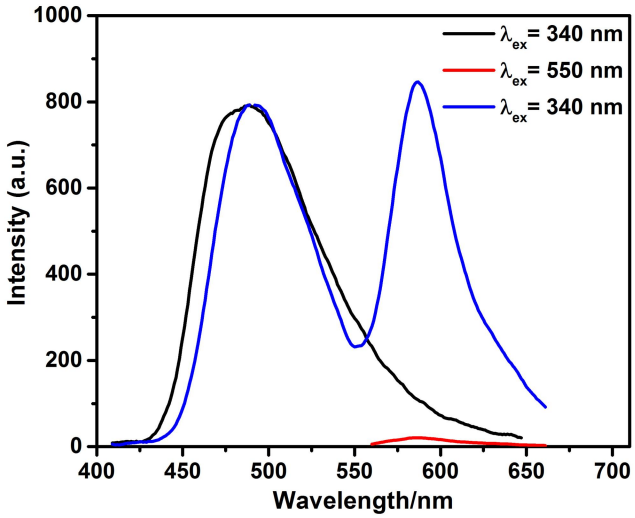

Figure S27. Gated spectra of CD-PY@CB[8]@RhB (1:0.5:0.02) under different excitation conditions in water, blue trace (λ_{ex} = 340 nm), red trace (λ_{ex} = 550 nm). The black trace represents the gated spectrum (λ_{ex}=340 nm) of CD-PY@CB[8], which was normalized according to the phosphorescence intensity at 490 nm of the blue trace ([CD-PY]= 5×10^{-4} M).

4. REFERENCES

(1) A. K. Rappé, C. J. Casewit, K. S. Colwell, W. A. Goddard III, W. A. Skiff, *J. Am. Chem. Soc*., 1992, **114**, 10024-10035.

(2) M. J. Frisch, G. W. Trucks, H. B. Schlegel, G. E. Scuseria,M. A. Robb, J. R. Cheeseman, G. Scalmani, V. Barone,G. A. Petersson, H. Nakatsuji, X. Li, M. Caricato, A. V. Marenich,J. Bloino, B. G. Janesko, R. Gomperts, B. Mennucci, H. P. Hratchian,J. V. Ortiz, A. F. Izmaylov, J. L. Sonnenberg, D. Williams-Young,F. Ding, F. Lipparini, F. Egidi, J. Goings, B. Peng, A. Petrone,T. Henderson, D. Ranasinghe, V. G. Zakrzewski, J. Gao, N. Rega,G. Zheng, W. Liang, M. Hada, M. Ehara, K. Toyota, R. Fukuda,J. Hasegawa, M. Ishida, T. Nakajima, Y. Honda, O. Kitao, H. Nakai,T. Vreven, K. Throssell, J. A. Montgomery, Jr., J. E. Peralta,F. Ogliaro, M. J. Bearpark, J. J. Heyd, E. N. Brothers, K. N. Kudin,V. N. Staroverov, T. A. Keith, R. Kobayashi, J. Normand,K. Raghavachari, A. P. Rendell, J. C. Burant, S. S. Iyengar,J. Tomasi, M. Cossi, J. M. Millam, M. Klene, C. Adamo, R. Cammi,J. W. Ochterski, R. L. Martin, K. Morokuma, O. Farkas,J. B. Foresman, and D. J. Fox, Gaussian 16, Revision A.03, Gaussian, Inc., Wallingford, CT, 2016.

(3) C. Y. Legault, CYLview, 1.0b, Université de Sherbrooke, Sherbrooke, Quebec, Canada, 2009, http://www.cylview.org.

(4) Z. Li, Y. Han, F. Wang, *Nat. Commun*., 2019, **10**, 3735.

(5) J.-J. Li, Y. Chen, J. Yu, N. Cheng, Y. Liu, *Adv. Mater*., 2017, **29**, 1701905.